Title
D7H-Test Results

Author
Caspi, S

Publication Date
1982-07-01

Lawrence Berkeley Laboratory
UNIVERSITY OF CALIFORNIA

Accelerator & Fusion Research Division

D7H-TEST RESULTS

S. Caspi

July 1982

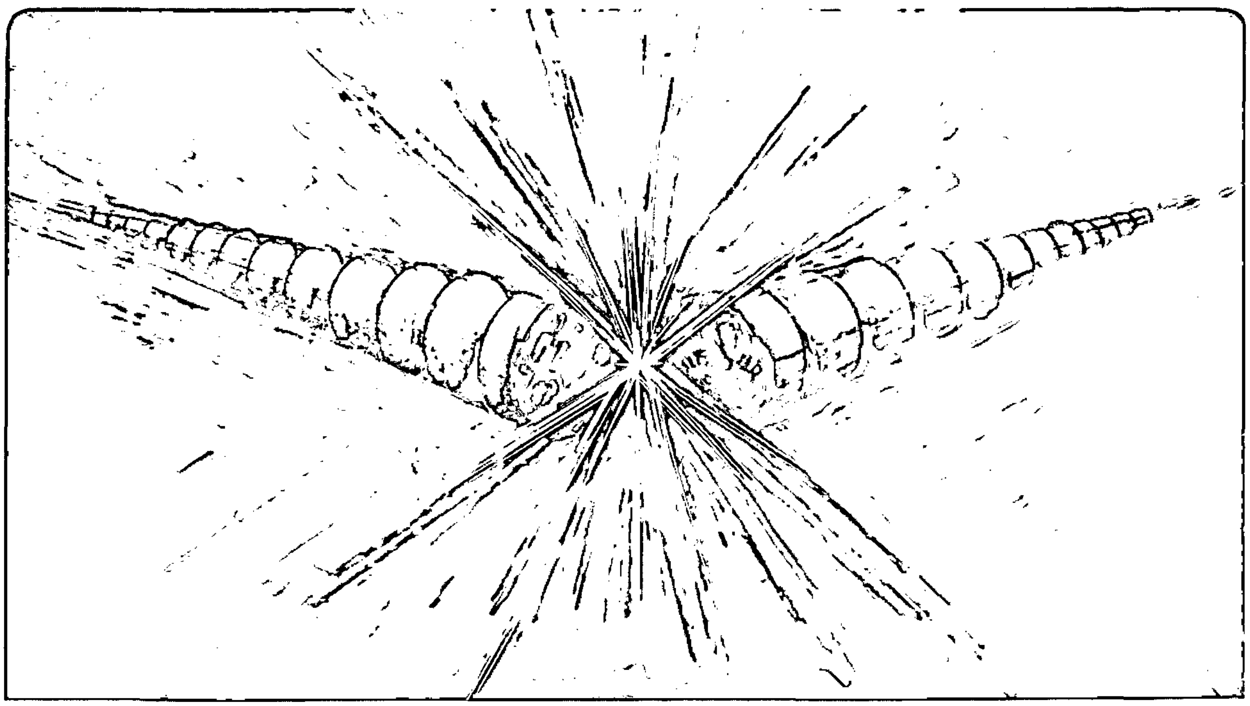

Prepared for the U.S. Department of Energy under Contract DE-AC03-76SF00098

DISCLAIMER

SUMAG-70
LBL-14796

D7H-Test Results*

S. Caspi

Accelerator and Fusion Research Division
Lawrence Berkeley Laboratory
University of California
Berkeley, California 94720

July 30, 1982

*This work was supported by the Director, Office of Energy Research, Office of High Energy and Nuclear Physics, High Energy Physics Div., U.S. Dept. of Energy, under Contract No. DE-AC03-76SF00098.

D7H-Test Results*

S. Caspi

Data was reduced from the voltage-time relations stored in files D7H001 to D7H090 on HP1000. The I-B calibration curve is included in Fig. 1. The data base is shown in Table 1 and can be used by the 9845B. The data include the quench location, Q_2 layer 1 top, Q_3 layer 1 bottom and the quench current and its normalized value with respect to short sample, I_c = 4920A at 4.4 K, I_c = 6710 A at 1.8 K. The resistance (Ω/cm) was calculated using the propogation time according to the voltage change across the measured sections. The conductor potential length are $L_{5,9}$ = 48.6 cm, $L_{6,10}$ = 17.9 cm, $L_{7,\ 11}$ = 40.6 cm (Fig. 8). The turn to turn velocity V_t was calculated dividing the nominal turn to turn distance (58 mil) by the propagation time (Trans. Time). The quench time T_q was measured from the time the resistive rise starts until the energy extraction system fires. Figures 2-6 are plots of the data base. The time to energy extracton can be estimated as:

$$T_q = \frac{Vo}{2IR'V} \tag{1}$$

where:

Vo = trip voltage

R' = resistance per unit length

V = velocity

I = current

For a propagation which is axial only. The discontinity in T_q (Fig. 4) is due to a drop in the propagation velocity when the temperature was

*This work was supported by the Director, Office of Energy Research, Office of High Energy and Nuclear Physics, High Energy Physics Div., U.S. Dept. of Energy, under Contract No. DE-AC03-76SF00098.

lowered from 4.4 K to 1.8 K. Assuming Vo = .25 volt and using I, R', V values from the data base, equation 1 is plotted in Fig 5.

Resistivity

The resistance per unit length at the normal state is plotted in Fig. 6. The values at the magnet ends vary from .9 to 1.3 $\mu\Omega$/cm between 4000A and 7000 A and the straight section values are about 15 percent higher. For a 23 strand cable at 27 mil strand diameter and 1.8/1 S.C/copper ratio the total copper cross section area is 5.46×10^{-2} cm^2. Assuming all the current had been switched to the copper the resistivity is 4.9×10^{-8} – 7.1×10^{-8} (Ω cm) and the corresponding resistivity ratio is therefore RRR = 35 to 20.

The alteration of the quench location between the halves of the inner shell is plotted in Fig.7 and the quench origin around the first inner turn is plotted in Fig. 8. All quenches occured around the first turn! (The only exceptions were very fast ramp rates).

Temperature Rise

After the normal zone propagates through a measured section, its resistance keeps increasing due to a temperature increase. The resistance rise with respect to time is observed to be linear (Fig. 9) in the time scale before the energy extraction. Converting this values to a resistivity rise the results are given in Table 2. A simplified energy balance result in an approximate temperature-time relation.

$$MC\frac{dT}{dt} = I^2R \qquad (2)$$

$M = \rho_d\, lA$ (ρ_d = density, l = length, A = crossection area)

$R = \rho_r\, l/A$ (ρ_r= resistivity)

The total mass assumes copper only (e.g. no liquid participation).

Equation (2) reduces to

$$C\,\frac{dT}{dt} = \frac{\rho_r}{\rho_d}\,\frac{I^2}{A^2}$$

$$\int C\,dT = \frac{I^2}{A^2}\,\frac{1}{\rho_d}\int \rho_r\,dt$$

The experiment shows that $\rho_r = \rho_r(t) = \alpha t$

therefore,

$$\int C\,dT = \frac{\alpha}{2\rho_d}\left(\frac{It}{A}\right)^2 \tag{3}$$

Equation (3) was solved for 2 nominal cases using $A = 5.46 \times {}^{-10}\ cm^2$; $\rho_d = 8.94\ (gr/cm^3)$

1. File = D7H008 (4.4 K)

   $I = 4220\ A;$

   $\alpha = 1.1 \times 10^{-6}\ \Omega\text{-cm/sec}$

   $\int C\,dT = 3.675 \times 10^{-4} . t^2$ (t = msec)

2. File = D7H061 (2.0 K)

   $I = 6340\ A;$

   $\alpha = 2.46 \times 10^{-6}\ \Omega\text{-cm/sec}$

   $\int C\,dT = 1.855 \times 10^{-3} . t^2$ (t = msec)

The result from the two cases using integral values of specific heat for copper are shown in Fig. 10.

Magnet Rate Dependance and Losses

The magnet was ramped at various rates and the quench field recorded. Repeating the test both in the He I and He II result in the relations shown in Fig. 11. The normalized field data were then fitted to a parabolic relation and plotted in Fig. 12.

Using our standard procedure in He II to determine energy losses the average heat flux generated during a cycle is plotted in Fig. 13 for a number of different field rates.

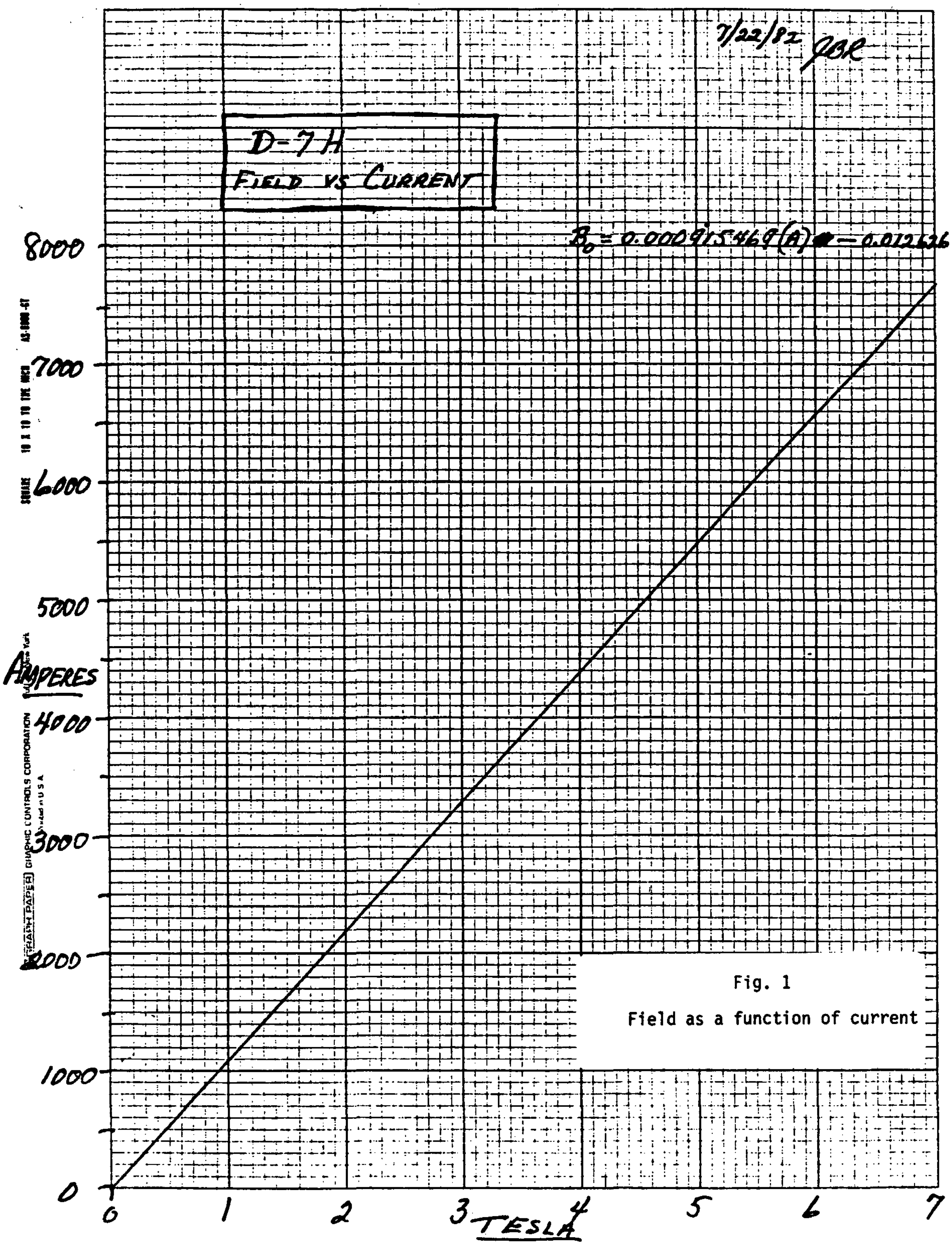

Fig. 1

Field as a function of current

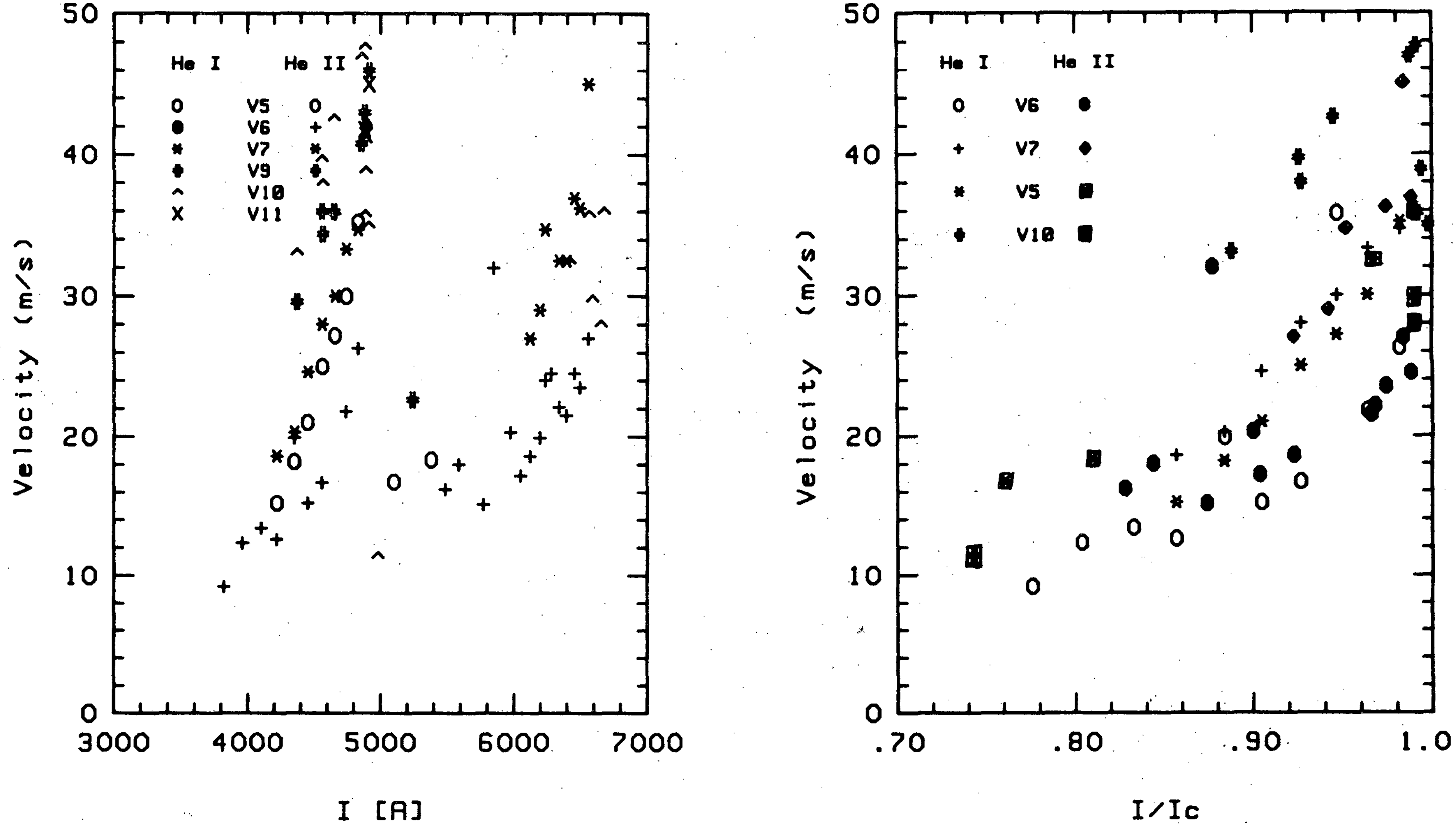

Fig. 2 Axial Velocity

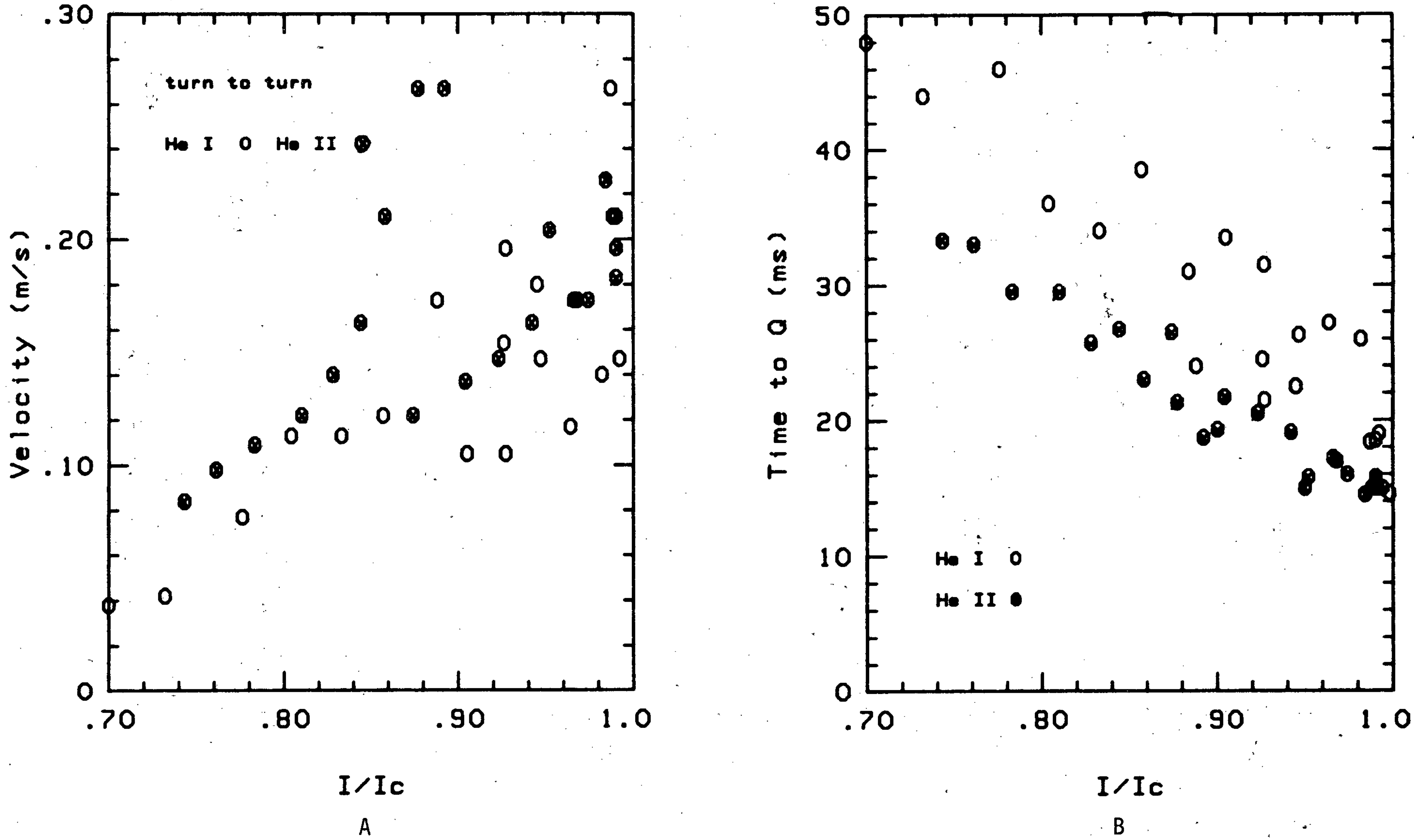

Fig. 3: A) Turn to turn velocity; B) Time from initial resistive rise to energy extraction as a function of normalized current.

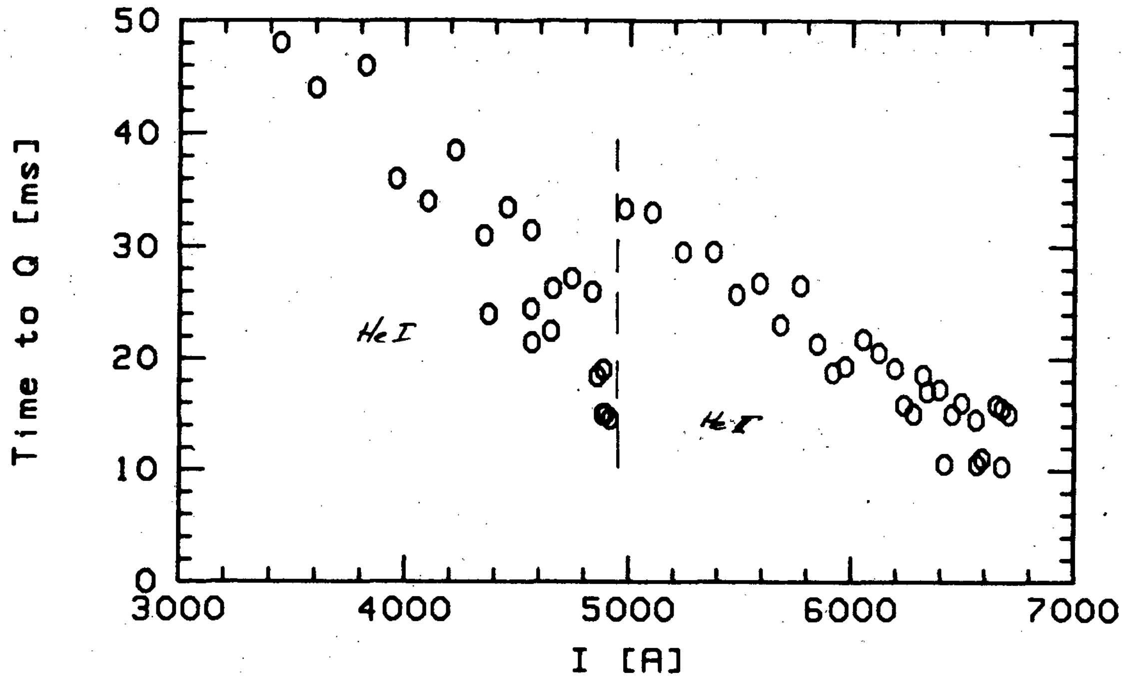

Fig. 4 Measured time from detection to extraction as a function of current.

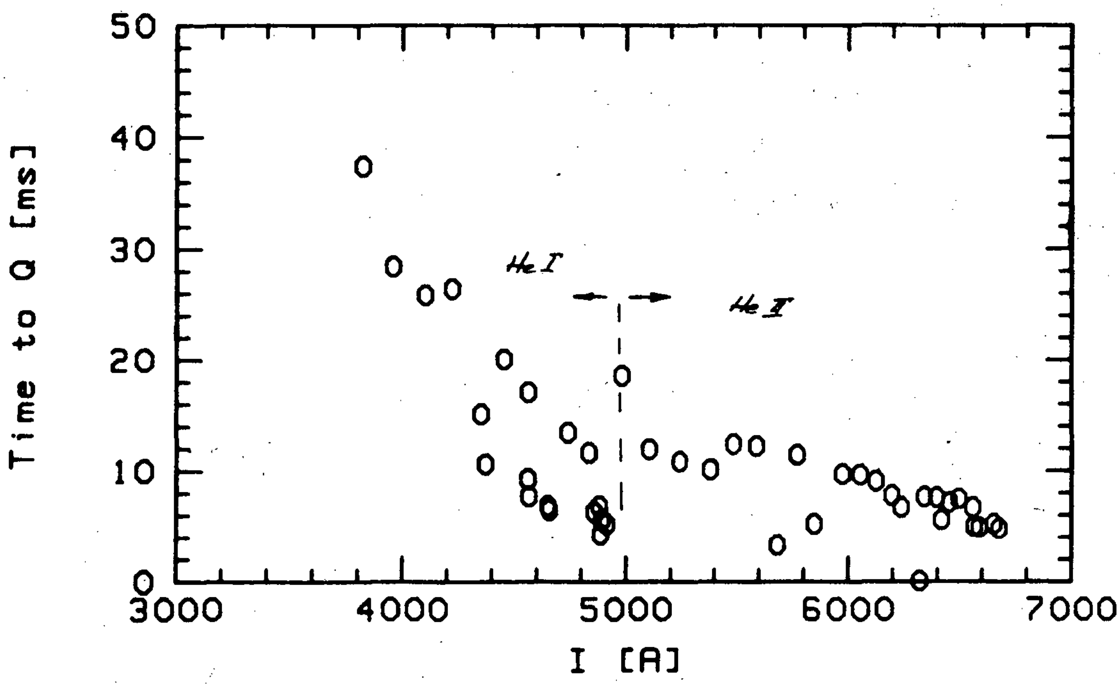

Fig. 5 Calculated time to extraction based on Equation 1 using the same data points.

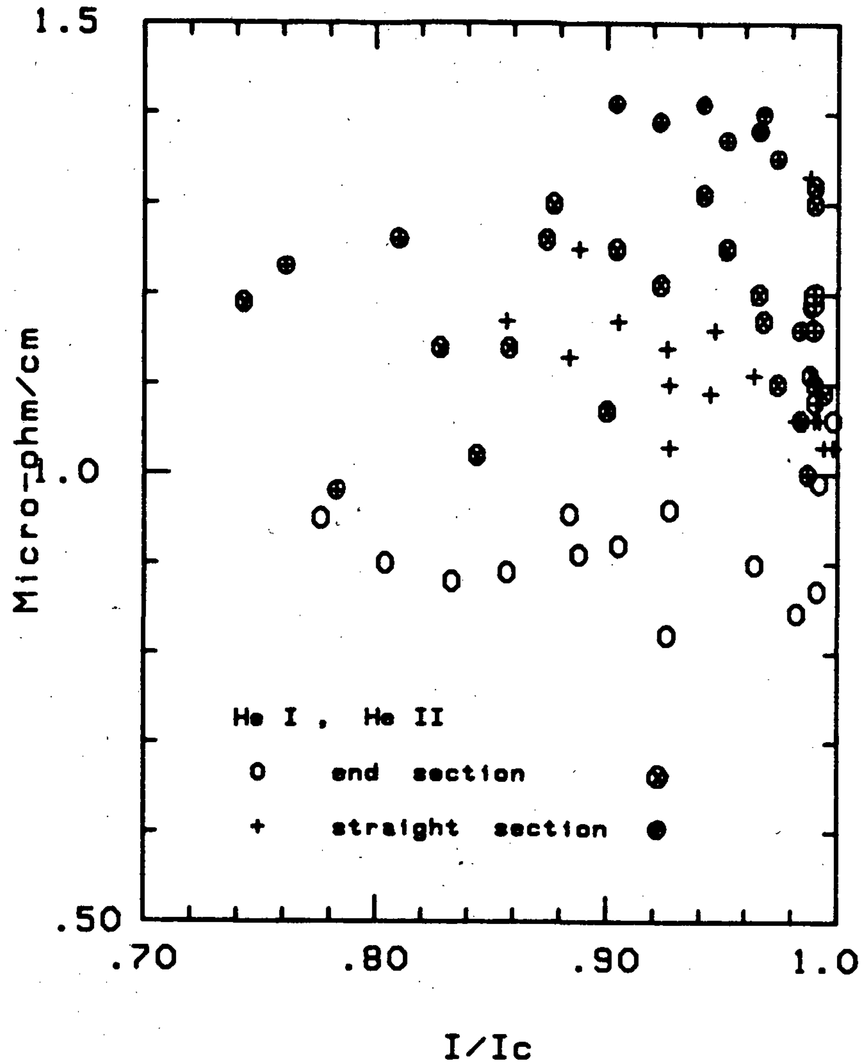

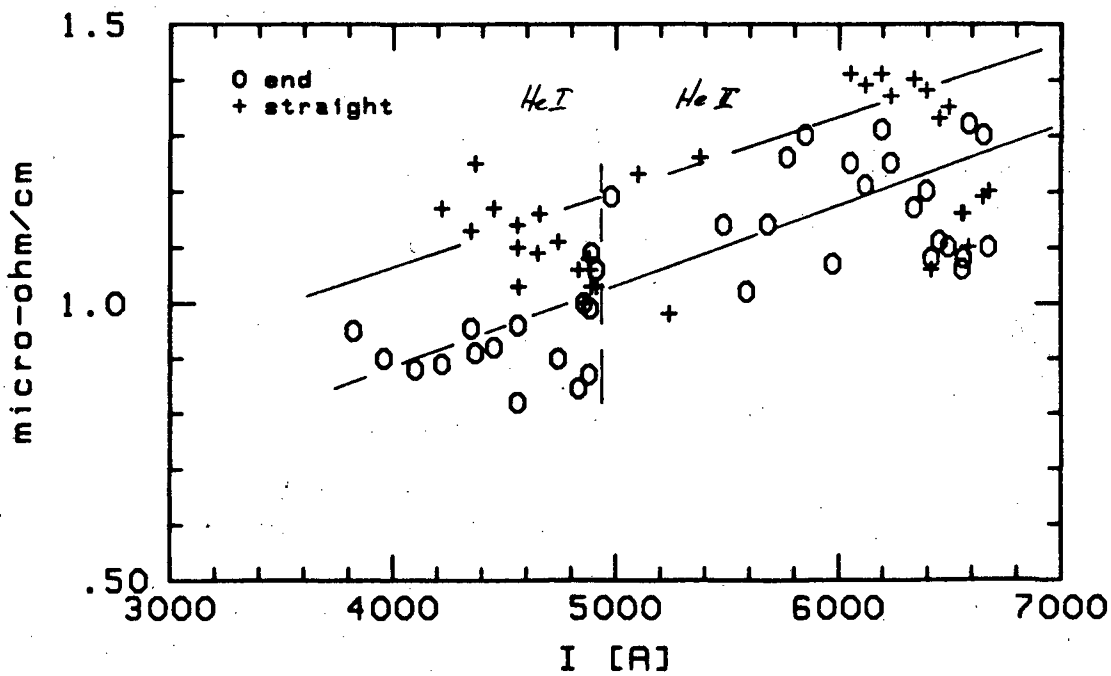

Fig. 6 Resistance per unit length during the transition from the S.C. state to the normal state.

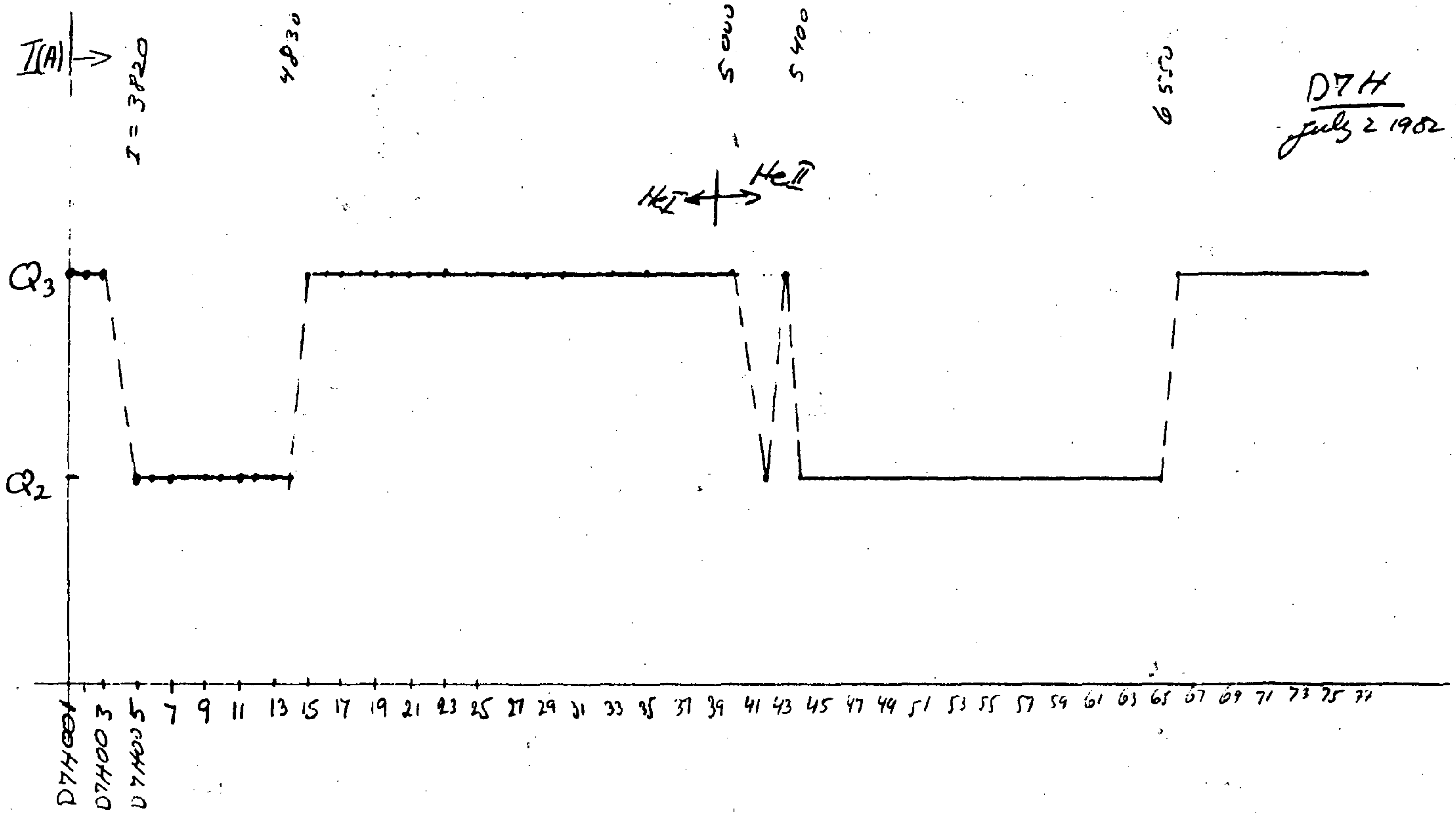

Fig. 7 Quench location variation per half inner shell as a function of storage file.

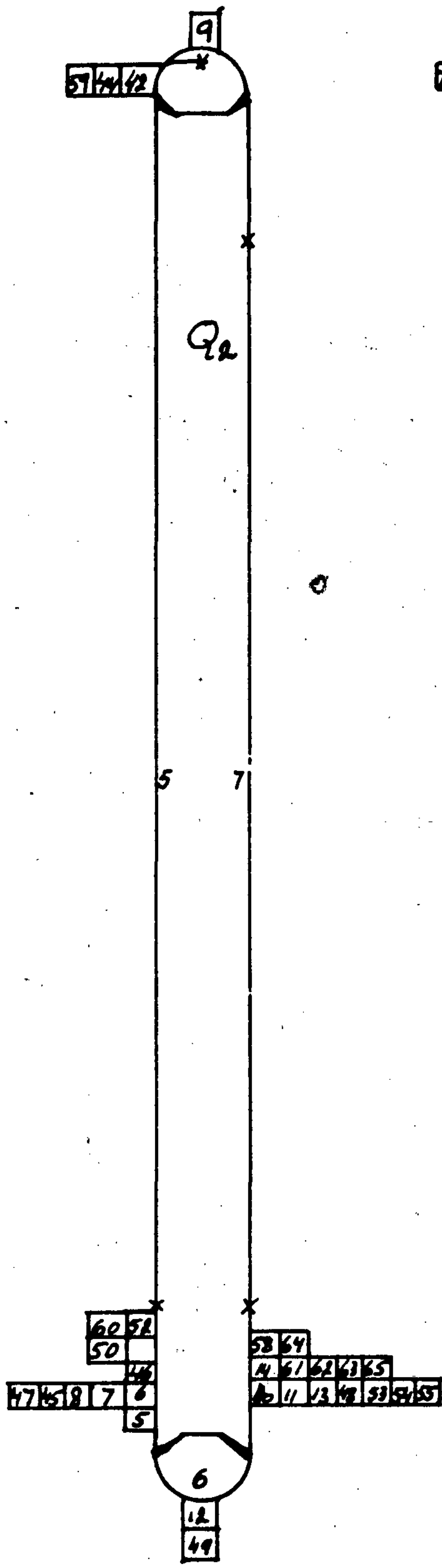

Fig. 8 Quench location in upper and lower inner shell.

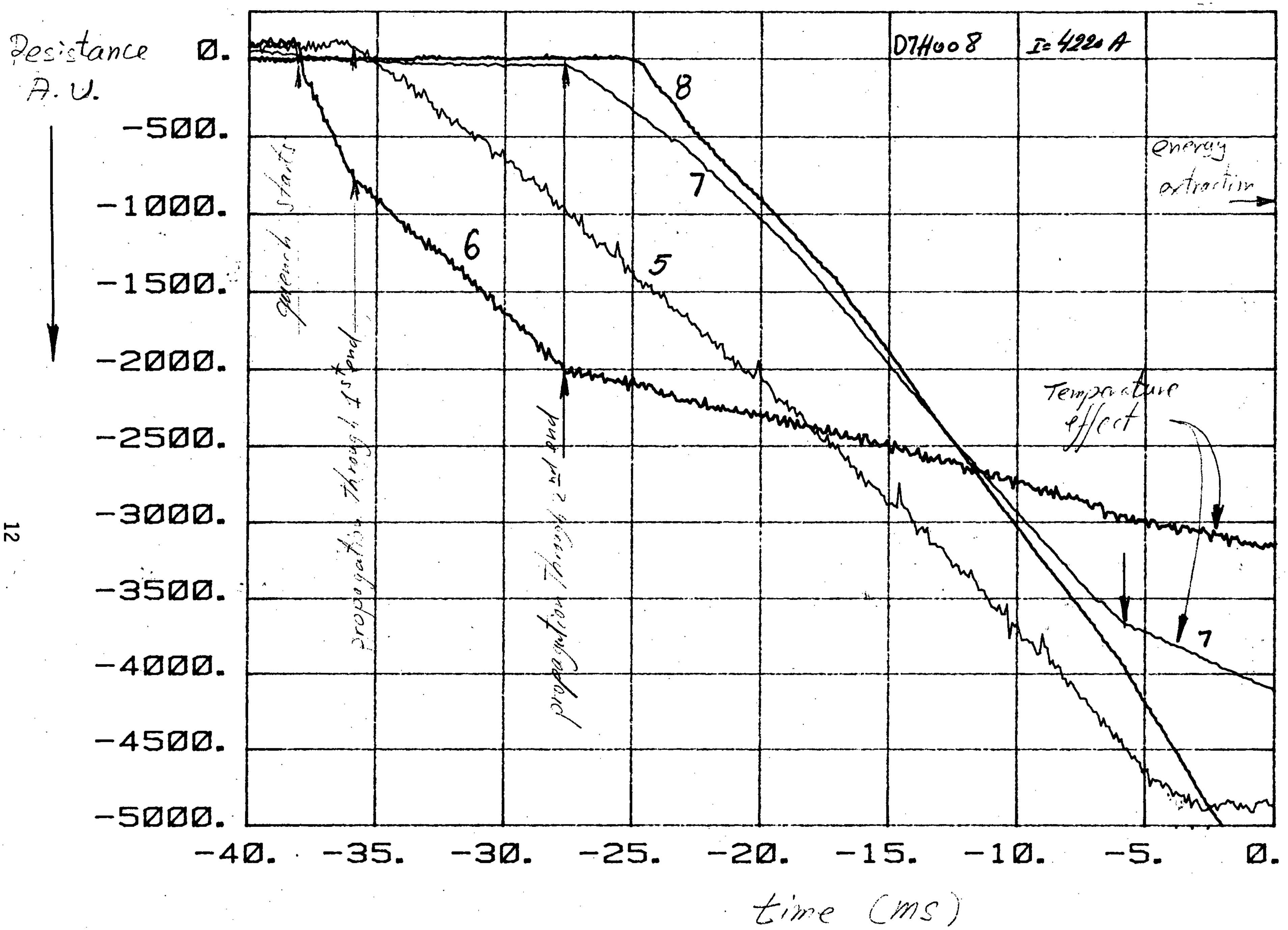

Fig. 9 Normal zone propagation and resistive rise prior to energy extraction.

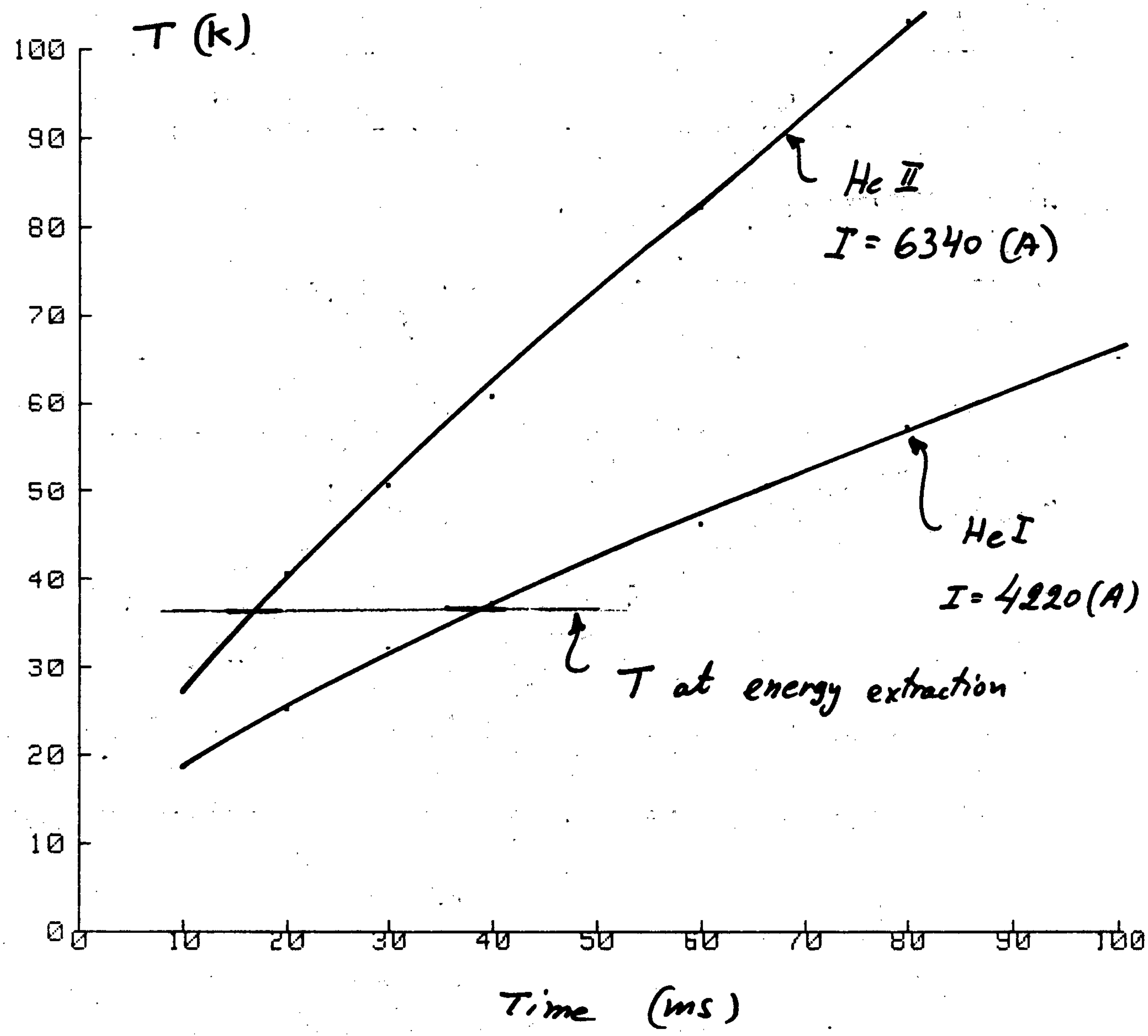

Fig. 10 Temperature history prior to energy extraction based on equation 3.

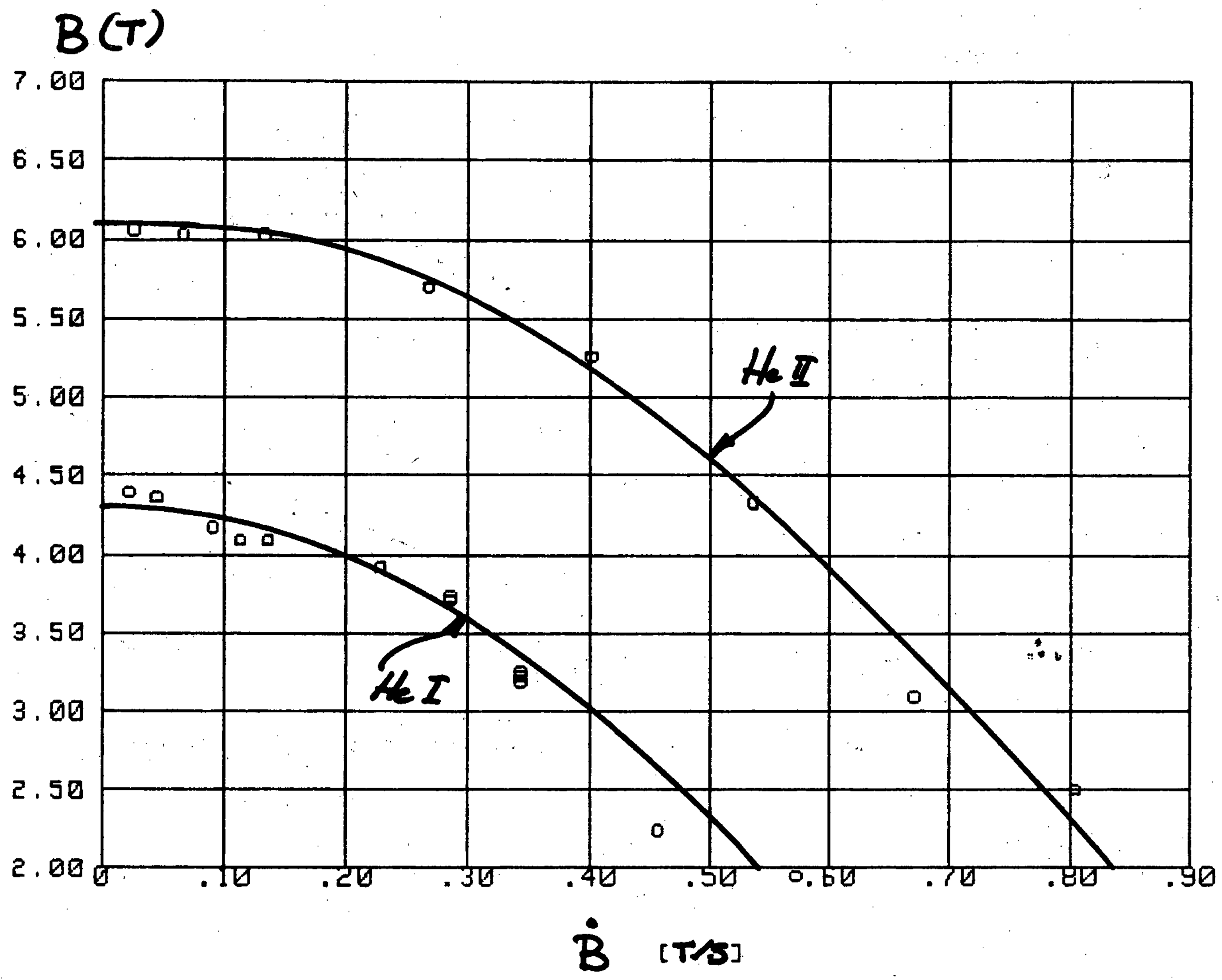

Fig. 11 Maximum field as a function of ramp rate.

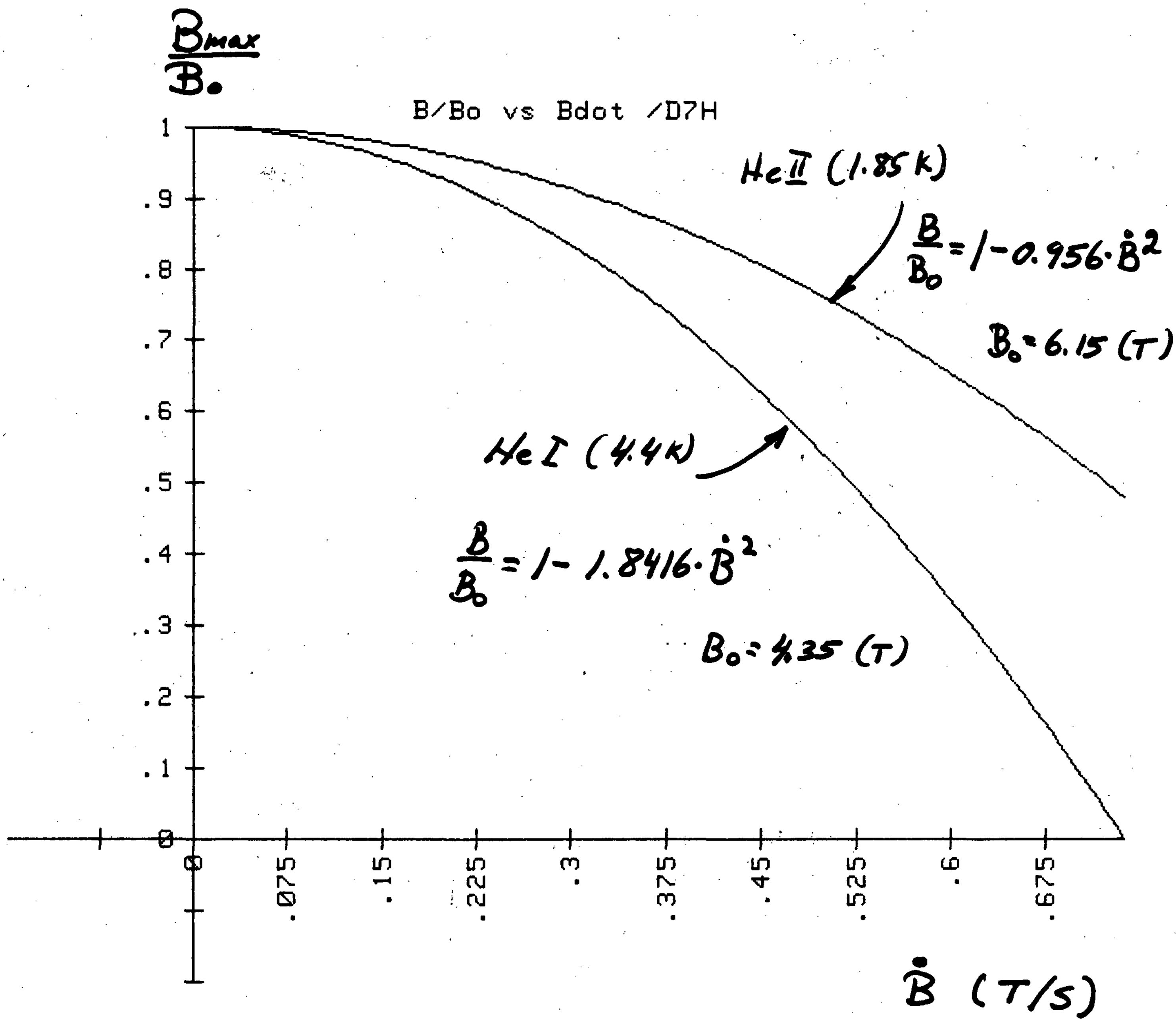

Fig. 12 Normalized maximum field as a function of ramp rate. The lines are a least fit to the data.

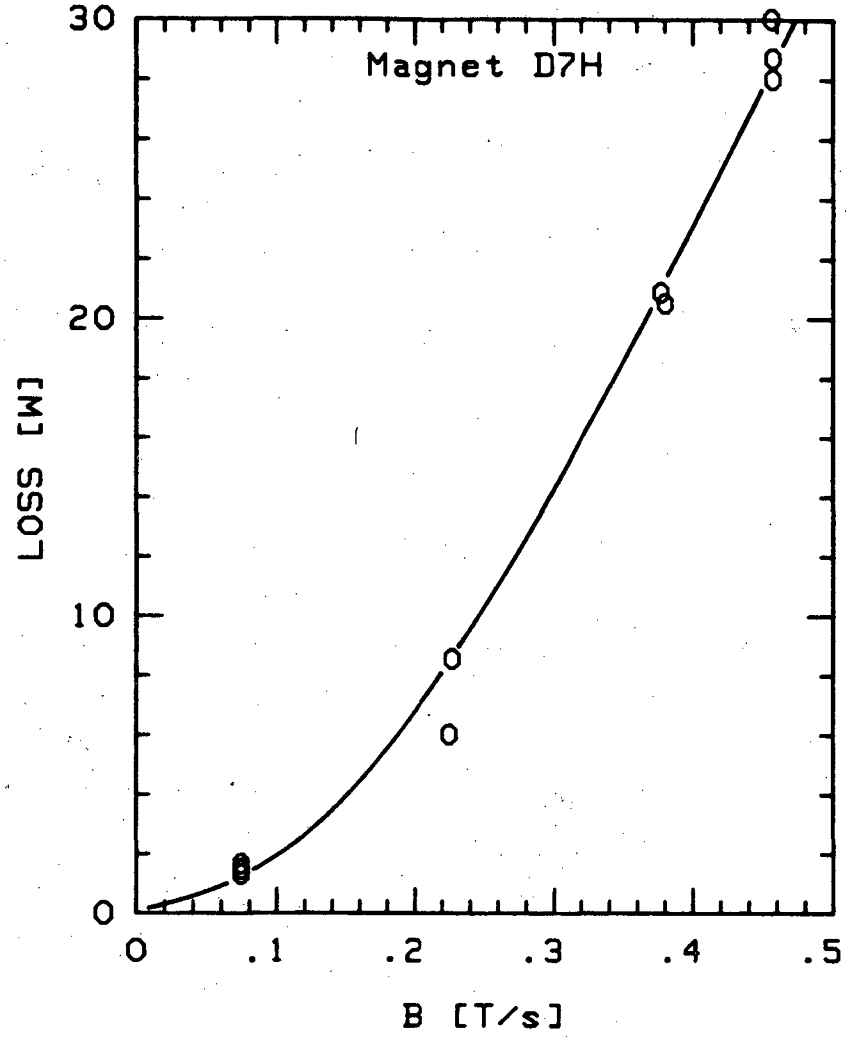

Fig. 13 Magnet loss during cycling around 0-3.85 (T).

FILE NAME	LOCATION	Iq (A)	Tq (ms)	T (K)	Iq/Ic	MICROHM/CM (end)	MICROHM/CM (straight)	V5 (m/s)	V6 (m/s)	V7 (m/s)	V9 (m/s)	V10 (m/s)	V11 (m/s)	Vt (m/s)	TRANS. TIME (ms)
D7H001		0	0.0	0.00	0.000	0.00	0.00	0.0	0.0	0.0	0.0	0.0	0.0	0.000	0.0
D7H002	Q3	3444	40.0	4.40	.700	0.00	0.00	0.0	0.0	0.0	0.0	0.0	0.0	.030	30.0
D7H003	Q3	3603	44.0	4.40	.732	0.00	0.00	0.0	0.0	0.0	0.0	0.0	0.0	.042	35.0
D7H005	Q2	3821	46.0	4.40	.776	.95	0.00	0.0	9.2	0.0	0.0	0.0	0.0	.077	19.0
D7H006	Q2	3959	36.0	4.40	.804	.90	0.00	0.0	12.3	0.0	0.0	0.0	0.0	.113	13.0
D7H007	Q2	4100	34.0	4.40	.833	.00	0.00	0.0	13.4	0.0	0.0	0.0	0.0	.113	13.0
D7H008	Q2	4220	30.5	4.40	.857	.89	1.17	15.2	12.6	10.6	0.0	0.0	0.0	.122	12.0
D7H009	Q2	4351	31.0	4.40	.884	.96	1.13	10.2	19.9	20.3	0.0	0.0	0.0	1.470	1.0
D7H010	Q2	4453	33.5	4.40	.905	.92	1.17	21.0	15.2	24.6	0.0	0.0	0.0	.105	14.0
D7H011	Q2	4561	31.5	4.40	.927	.96	1.10	25.0	16.7	20.0	0.0	0.0	0.0	.105	14.0
D7H012	Q2	4650	26.3	4.40	.947	0.00	1.16	27.2	35.0	30.0	0.0	0.0	0.0	.147	10.0
D7H013	Q2	4742	27.2	4.40	.964	.90	1.11	30.0	21.0	33.3	0.0	0.0	0.0	.117	12.5
D7H014	Q2	4833	26.0	4.40	.982	.05	1.06	35.2	26.3	34.7	0.0	0.0	0.0	.140	10.5
D7H015	Q3	4913	14.6	4.40	.990	1.06	1.03	0.0	0.0	0.0	46.0	35.0	45.0	1.130	1.3
D7H016	Q3	4880	15.0	4.40	.991	.07	1.00	0.0	0.0	0.0	43.0	47.7	41.0	3.000	.5
D7H017	Q3	4891	15.0	4.40	.994	1.09	1.03	0.0	0.0	0.0	42.0	30.9	41.4	3.000	.5
D7H018	Q3	4885	19.0	4.40	.992	.99	1.06	0.0	0.0	0.0	60.7	35.0	59.7	.147	10.0
D7H019	Q3	4857	10.4	4.40	.987	1.00	1.00	0.0	0.0	0.0	40.0	47.0	0.0	.267	5.5
D7H020	Q3	4650	22.5	4.40	.945	0.00	1.09	0.0	0.0	0.0	36.0	42.6	0.0	.180	0.0
D7H021	Q3	4559	24.5	4.40	.926	.02	1.14	0.0	0.0	0.0	36.0	39.7	0.0	.154	9.5
D7H022	Q3	4564	21.5	4.40	.927	0.00	1.03	0.0	0.0	0.0	34.4	30.0	0.0	.196	7.5
D7H023	Q3	4370	24.0	4.40	.880	.91	1.25	0.0	0.0	0.0	29.6	33.1	0.0	.173	8.5
D7H040	Q3	4900	33.3	1.05	.743	1.19	0.00	0.0	0.0	0.0	0.0	11.4	0.0	.084	17.5
D7H042	Q2	5102	33.0	1.05	.761	0.00	1.23	16.0	0.0	0.0	0.0	0.0	0.0	.090	15.0
D7H043	Q3	5240	29.5	1.07	.783	0.00	.98	0.0	0.0	0.0	22.6	0.0	0.0	.109	13.5
D7H044	Q2	5300	29.5	1.90	.810	0.00	1.26	10.3	0.0	0.0	0.0	0.0	0.0	.122	12.0
D7H045	Q2	5484	25.7	1.90	.828	1.14	0.00	0.0	16.2	0.0	0.0	0.0	0.0	.140	10.5
D7H046	Q2	5507	26.7	1.90	.844	1.02	0.00	0.0	18.0	0.0	0.0	0.0	0.0	.163	9.0
D7H047	Q2	5682	23.0	1.90	.858	1.14	0.00	0.0	59.6	0.0	0.0	0.0	0.0	.210	7.0
D7H048	Q2	5769	26.5	1.95	.874	1.26	0.00	0.0	15.1	0.0	0.0	0.0	0.0	.122	12.0
D7H049	Q2	5847	21.3	1.85	.877	1.30	0.00	0.0	32.0	0.0	0.0	0.0	0.0	.267	5.5
D7H050	Q2	5917	10.7	1.89	.892	0.00	0.00	0.0	99.0	0.0	0.0	0.0	0.0	.267	5.5
D7H052	Q2	5973	19.3	1.91	.900	1.07	0.00	0.0	20.3	0.0	0.0	0.0	0.0	.470	3.1
D7H053	Q2	6051	21.7	1.83	.904	1.25	1.41	0.0	17.2	0.0	0.0	0.0	0.0	.137	10.7
D7H054	Q2	6122	20.5	1.89	.923	1.21	1.39	0.0	18.6	27.0	0.0	0.0	0.0	.147	10.0
D7H055	Q2	6194	19.1	1.99	.942	1.31	1.41	0.0	19.9	29.0	0.0	0.0	0.0	.163	9.0
D7H058	Q2	6236	15.0	2.00	.952	1.25	1.37	0.0	24.0	34.7	0.0	0.0	0.0	.204	7.2
D7H060	Q2	6279	15.0	1.80	.958	0.00	0.00	0.0	24.5	0.0	0.0	0.0	0.0	.590	2.5
D7H061	Q2	6340	17.0	2.00	.960	1.17	1.40	0.0	22.1	32.5	0.0	0.0	0.0	.173	8.5
D7H062	Q2	6395	17.2	1.90	.966	1.20	1.30	0.0	21.5	32.5	0.0	0.0	0.0	.173	8.5
D7H063	Q2	6453	15.0	2.04	.988	1.11	1.33	0.0	24.5	36.9	0.0	0.0	0.0	.210	7.0
D7H064	Q2	6495	16.0	1.85	.974	1.10	1.35	0.0	23.5	36.2	0.0	0.0	0.0	.173	8.5
D7H065	Q2	6558	14.5	1.80	.984	1.06	1.16	0.0	27.0	45.0	0.0	0.0	0.0	.226	6.5
D7H066	Q3	6587	11.0	2.03	.990	1.32	1.10	0.0	0.0	0.0	0.0	29.0	67.0	3.000	.5
D7H067	Q3	6417	10.5	2.14	.990	1.00	1.06	0.0	0.0	0.0	0.0	32.5	62.5	3.000	.5
D7H068	Q3	6652	15.0	1.07	.990	1.30	1.19	0.0	0.0	0.0	0.0	20.0	60.0	.196	7.5
D7H069	Q3	6564	10.5	2.05	.990	1.00	1.16	0.0	0.0	0.0	0.0	35.0	65.0	3.000	.5
D7H070	Q3	6709	15.0	1.01	.990	0.00	0.00	0.0	0.0	0.0	0.0	0.0	54.0	.196	7.5
D7H071	Q3	6675	10.3	1.89	.990	1.10	0.00	0.0	0.0	0.0	0.0	36.0	62.0	3.000	.5
D7H072	Q3	6670	15.5	0.00	.998	0.00	1.20	0.0	0.0	0.0	0.0	0.0	0.0	.210	7.0
D7H073	Q3	6320	10.5	0.00	.990	0.00	0.00	0.0	0.0	0.0	0.0	0.0	0.0	.103	0.0

Table I. Data base on the 9845B desktop; I_q = quench current; T_q = time from quench detection to energy extraction; I_q/I_c = normalized quench current; Microhm/cm = resistive rise from S.C. state to normal state per unit length; V_i = propagation velocity for section i; V_t = turn to turn velocity; Trans. time = turn to turn propagation time.

File name	Resistivity rise micro_ohm-cm/s end	straight
He I		
D7H005	1.00	-
D7H006	1.2	-
D7H007	0.97	-
D7H008	1.06	1.13
D7H009	1.21	0.99
D7H010	1.40	1.13
D7H011	1.27	1.23
D7H012	1.40	1.18
D7H013	1.31	1.36
D7H014	1.40	1.33
D7H015	1.34	-
D7H016	1.13	-
D7H017	1.21	1.04
D7H018	1.10	1.15
He-II		
D7H040	1.43	-
D7H045	1.52	-
D7H046	2.12	-
D7H047	2.12	-
D7H048	2.65	-
D7H049	2.31	-
D7H050	2.13	-
D7H052	1.67	-
D7H053	2.53	-
D7H054	2.71	-
D7H055	2.56	-
D7H058	2.02	-
D7H060	2.34	-
D7H061	2.46	-
D7H062	2.78	-
D7H063	3.11	-
D7H064	3.05	-
D7H065	2.65	-

Table 2 Resistivity per second prior to energy extraction due to temperature rise only.

TECHNICAL INFORMATION DEPARTMENT
LAWRENCE BERKELEY LABORATORY
UNIVERSITY OF CALIFORNIA
BERKELEY, CALIFORNIA 94720